November 3, 2003

PROPOSAL: Feasibility study of a polarized $^6Li^{3+}$ ion source

SPOKESPERSON:

Name	Kichiji Hatanaka
Institution	RCNP, Osaka University,
Address	10-1 Mihogaoka, Ibaraki, Osaka 567-0047
Phone number	+81-6-6879-8928
FAX number	+81-6-6879-8928
E-mail	hatanaka@rcnp.osaka-u.ac.jp

Collaborators:

Name	Institution	Title or Position
A. Tamii	RCNP Osaka University	Associate Professor
Y. Sakemi	RCNP Osaka University	Associate Professor
Y. Shimizu	RCNP Osaka University	D2
K. Fujita	RCNP Osaka University	D1
Y. Tameshige	RCNP Osaka University	M2
H. Okamura	CYRIC Tohoku University	Professor
T. Wakasa	Kyushu University	Associate Professor
T. Uesaka	CNS University of Tokyo	Lecturere
T. Wakui	CNS University of Tokyo	Research Associate
T. Nakagawa	RIKEN	Researcher

BUDGET: Experimental expenses 14,500,000 yen

1 Scientific motivation

Recently, it has become possible to calculate nuclear properties based on the realistic potentials or chiral perturbation theory and a lot of attensions are arized to understand the nuclear physics from the fundamental interactions. In these calculations it is found essential to explicitly treat pions in nuclei. Yukawa showed the nucleon-nucleon (NN) interaction is mediated by pions for the first time in 1935 [1]. However, pions have not been explicitly included in such a nuclear physics theory as a shell model for a long period, where NN interactions are parametrized to explain nuclear phenomena. One of the most prominent features of the pion exchange interaction is the strong tensor force which binds a n-p pair to a deuteron. The pionic field in nuclei is largely related to spin and isospin correlations in nuclei and many studies have been performed both experimentally and theoretically. Today, there are renewed interests on this subject.

At RCNP, the study of spin and isospin excitations is one of the main research programs and many experimental works have been performed with high quality beams and such sophisticated detection systems as magnetic spectrometers Grand Raiden and LAS, neutron Time of Flight facility NTOF, the (n,p) facility, and so on. These measurements have been performed with beams of polarized protons and deuterons, secondary polarized neutrons, unpolarized ^{3}He and ^{6,7}Li. Spin observables have provided inevitable information. Studies with polarized nuclear beams are expected to give opportunities to obtain much profound knowledges in spin isospin properties of nuclei. It has been shown recently that the tensor analyzing power A_{zz} of the (d,^{2}He) reaction has the extreme value at 0° [2]. This feature is model independent and valid for reactions having a spin parity structure of $1^+ + 0^+ \rightarrow 0^+ + I^\pi$. This tool is very efficient to investigate 0^- states embedded in the high excitation energy region of residual nuclei. 0^- states are typically interesting because they have the same spin and parity as pions and are expected to give information on pionic correlations in nuclei. The (^{6}Li,^{6}He) reaction with polarized ^{6}Li particles gives the good opportunity to investigate this subject. At RCNP, ^{6}Li particles can be accelerated up to 100 MeV/u where the NN spin isospin interaction becomes prominent. By the (^{6}Li,^{6}He) reaction, the Grand Raiden makes it possible to measure excitation energies and cross section with much better resolution and higher efficiency than by the (d,^{2}He) reaction. ^{6}He nucleus is unstable but has a long enough life time of 800 ms. On the other hand, ^{2}He is in the unbound state of two protons. If polarized ^{3}He beam becomes available, (^{3}He,t) measurements provide a more rich information than (p,n) experiments owing to the high resolution. With polarized nuclear beams, it is also possible to investigate spin dependent nucleus-nucleus interactions. These studies have been performed at lower energies, because there are no available polarized ion sources to produce intermediate energy polarized nuclei heavier than ^{3}He.

In this proposal, we would like to make feasibility tests to produce a polarized $^6Li^{3+}$ beam which can be accelerated by the RCNP ring cyclotron.[6] Li^{1+} particles are polarized by the direct optical pumping and subsequently fully ionized in the Electron Cyclotron Resonance (ECR) ionizer. A short history of polarized Li ion sources is summarized in Sec. 2. The proposed source and possible depolarization problems are discussed in Sec. 3. In Sec. 4, plans for the feasibility tests are described. The schedule and the budget requests are also summarized in Sec. 4.

2 Existing polarized Li sources

A pioneering work was performed in Hamburg [3] and the developed source was operated at the Hidelberg EN tandem accelerator [4, 5] which is shown in Fig. 1. It follows the atomic beam principle and consists of a lithium oven to produce Li atoms, a 6-pole magnet to select electron spin direction, a low field RF transition to transfer the electron polarization to the Li nucleus, a surface ionizer to get $^6Li^{1+}$ ions and a potacium channel to produce negative ions by charge exchange collisions. The typical polarization was about 65 % on the target for the accelerated beams of $^6Li^{3+}$ ions [5]. Similar sources were constructed at University of Wisconsin [6] and the Nuclear Structure Facility in Daresbury Laboratory [7]. An atomic beam source constructed for the Hidelberg MP tandem accelerator was improved by using an electro-optically modulated (EOM) laser beam for optical pumping [8]. The dye laser optically pumped polarized ^{6,7}Li source was constructed at Florida State University [9]. The schematic diagram of the source is shown in Fig. 2 and beam polarizations were reported to be 70-80 % or higher for optical pumping sources.

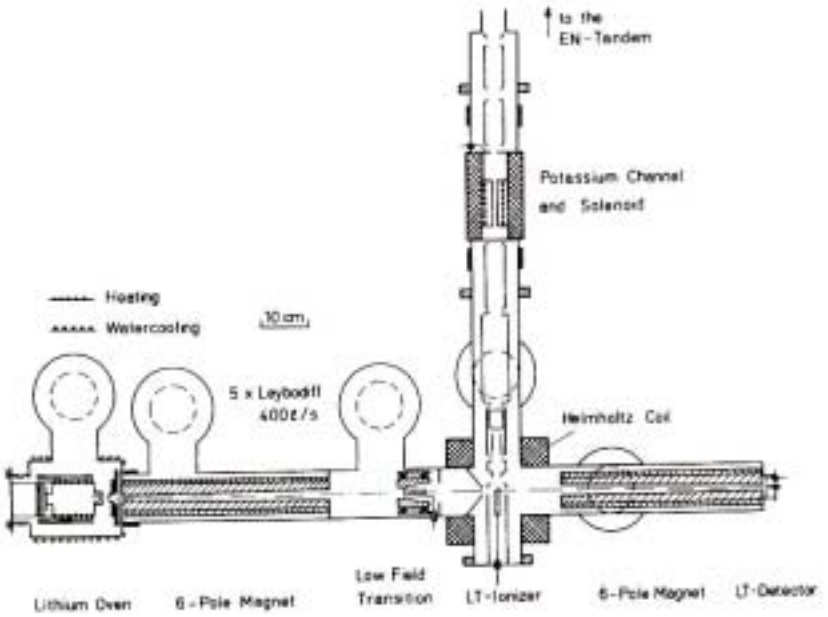

Figure 1: Schematic diagram of the ion source for a vector polarized $^6Li^-$ beam at the Heidelberg EN-tandem [3].

Sources mentioned above were operated at tandem accelerators. They provide Li^{1+} and Li^- ions which have even number of electrons. Electron spins are expected to be coupled to zero and depolarization may be avoided. There is a report to produce polarized $^6Li^{3+}$ beam at SATURNE [10]. The Li^{1+} ions are trapped and ionized inside the EBIS electron beam. The tensor polarization was measured to be 70 % at 187.5 keV/A after a RFQ. Depolarization effects were small owing to the short confinement time 3 ms to ionize Li^{1+} ions into Li^{3+} by multiple electron collisions and the large

magnetic field value 5 T to decouple the 1S electron and nuclear spin [10]. Figure 3 shows the schematic view of the EBIS.

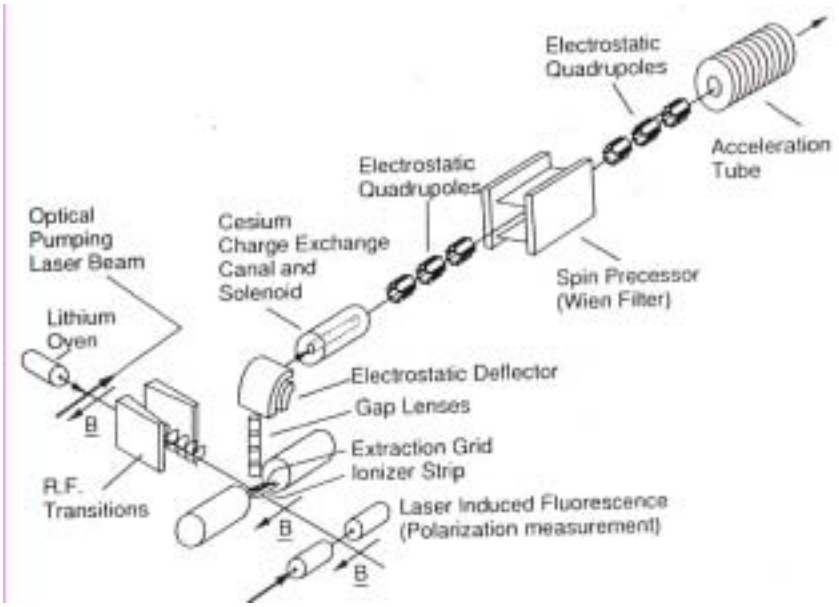

Figure 2: Schematic of the optically pumped polarized Li ion source at FSU [9].

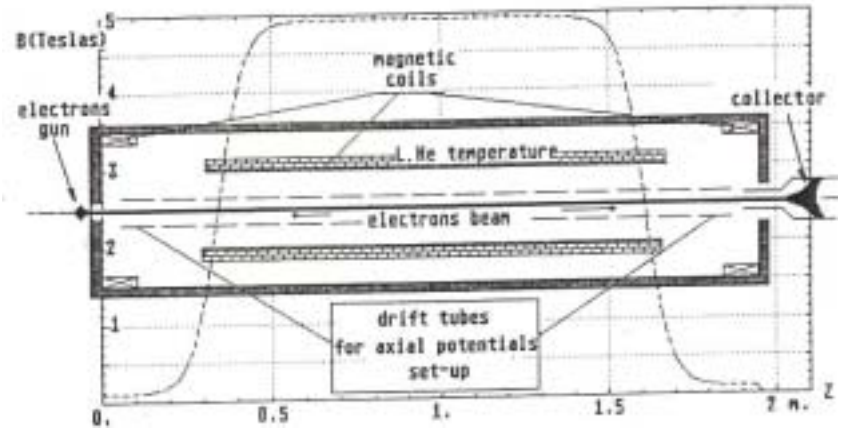

Figure 3: Schematic view of the EBIS (DIONÉ) at SATURNE to ionize Li^{1+} ion into Li^{3+} [10].

3 Estimation of depolarization of ^{6}Li nuclei in the ECR ionizer

We would like to propose a polarized $^6Li^{3+}$ source which utilizes an ECR ionizer to ionize $^6Li^{1+}$ ions into the 3+ state. The first part of the source has the same configuration as the FSU source [9]. ^{6}Li atoms are produced by an oven and optical pumped by diode lasers. Two diode laser systems are used to efficiently pump two $2S_{1/2}$ hyperfine states. Polarized atoms are ionized to singly charged $^6Li^{1+}$ ions by a surface ionizer and extracted by an electric field and introduced into an ECR plasma. Two electrons are removed in the ECR plasma. This is a kind of charge breeder of ISOL systems. The diagram of the source is shown in Fig. 4.

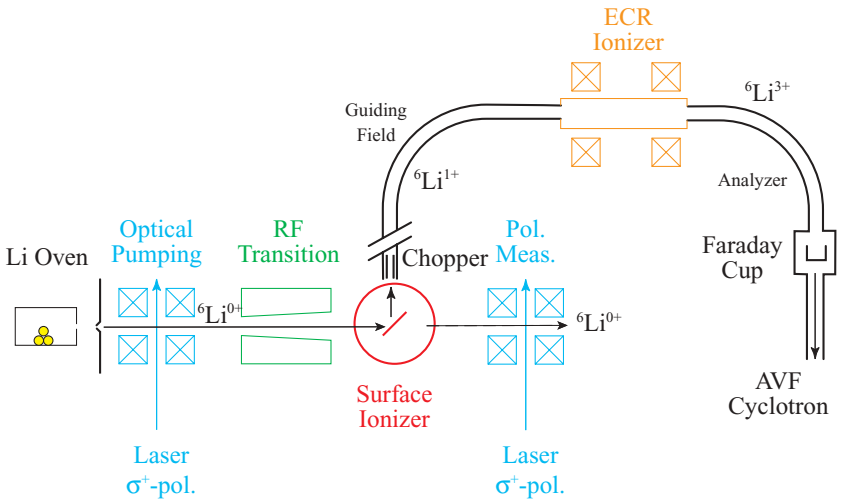

Figure 4: Schematic diagram of the proposed polarized $^6Li^{3+}$ source.

The polarization of ^{6}Li nuclei is anticipated to be reduced (depolarized) by many mechanisms in the ECR ionizer during the ionization processes . In this section we show results of the estimation of the possible depolarization. Note that the estimation largely depends on the plasma parameters which are usually not accurately known. Hence it is crucially important to perform test experiments to check and optimize the plasma parameters and to measure the depolarization. It is the purpose of this proposal.

Possible depolarization processes are summarized below. The authors thank Prof. M. Tanaka for listing up these processes.

1. Depolarization in the ionization process
2. Depolarization in the charge-exchange (electron capture) process
3. Depolarization in the atomic excitation and de-excitation process

4. Depolarization due to the electron spin resonance effect

5. Depolarization due to the inhomogeneity of the magnetic field

After briefly describing the assumed plasma condition, we show the estimation of depolarization for each process. By combining the estimated depolarization with the reaction rates, the total depolarization is calculated.

3.1 Assumption of the plasma condition

The plasma conditions in Table 1 are assumed in the calculation. The parameters are taken from the values which were fitted to the data measured by the laser ablation method for aluminum ions with a 14.5 GHz ECR ionizer (SHIVA) [11] at university of Tsukuba [14].

There exists a large ambiguity in estimating the confinement time of lithium ions. Here we scale the value, 10 msec, for Al^{13+} ions [14] by the following simply relation [14, 15]

$$\tau_i \propto i\sqrt{A}\,, \tag{1}$$

where τ_i is the confinement time of the ions, i is the charge state, and A is the mass. The estimated confinement times are

$$\tau_i = 0.33\, i \ \ \mathrm{msec}\,. \tag{2}$$

3.2 Depolarization in the ionization process

When an electron is stripped from a lithium atom or ion, depolarization of the lithium nucleus takes place since the pure $|J\,I>$ states are not the true eigenstates of the Hamiltonian, *i.e.* the hyperfine decoupling by the external magnetic field is imperfect.

3.2.1 $^6\mathbf{Li}^{0+} \rightarrow {}^6\mathbf{Li}^{1+}$ process

In this process, depolarization is negligible since the hyperfine coupling between the stripped electron (usually in the $2s$ shell) and the nucleus is small.

$$D_{0\rightarrow 1} = \mathbf{1}\,. \tag{3}$$

Table 1: Plasma conditions assumed in the calculation.

Electron Temperature	(T_e)	582	eV
Electron Density	(n_e)	2.23×10^{11}	cm^{-3}
Ion Temperature	(T_i)	5	eV
Buffer Gas		Oxgen	
Neutral Oxygen Density	(n_{gas})	1.44×10^{10}	cm^{-3}

3.2.2 $^6\mathrm{Li}^{1+} \rightarrow {}^6\mathrm{Li}^{2+}$ process

If an electron, which will be left in the following stripping process, and a ^{6}Li nucleus is initially in the $|IJ>$ state with a probability of $P(|IJ>)$, the time-averaged probability to find the $^6\mathrm{Li}^{2+}$ ion in the $P'(|I'J'>)$ state after stripping the other electron is expressed by the following matrix. Here I and J are the magnetic quantum number of the electron spin and the nucleus, respectively.

$$\begin{pmatrix} P'(|\uparrow +1>) \\ P'(|\uparrow\ \ 0>) \\ P'(|\uparrow -1>) \\ P'(|\downarrow -1>) \\ P'(|\downarrow\ \ 0>) \\ P'(|\downarrow +1>) \end{pmatrix} = \begin{pmatrix} 1 & 0 & 0 & 0 & 0 & 0 \\ 0 & \frac{1}{2}(1+\delta_+^2) & 0 & 0 & 0 & \frac{1}{2}(1-\delta_+^2) \\ 0 & 0 & \frac{1}{2}(1+\delta_-^2) & 0 & \frac{1}{2}(1-\delta_-^2) & 0 \\ 0 & 0 & 0 & 1 & 0 & 0 \\ 0 & 0 & \frac{1}{2}(1-\delta_-^2) & 0 & \frac{1}{2}(1+\delta_-^2) & 0 \\ 0 & \frac{1}{2}(1-\delta_+^2) & 0 & 0 & 0 & \frac{1}{2}(1+\delta_+^2) \end{pmatrix} \times \begin{pmatrix} P(|\uparrow +1>) \\ P(|\uparrow\ \ 0>) \\ P(|\uparrow -1>) \\ P(|\downarrow -1>) \\ P(|\downarrow\ \ 0>) \\ P(|\downarrow +1>) \end{pmatrix}$$

$$\begin{aligned} \delta_\pm &\equiv \frac{\pm\frac{1}{3}+x}{\sqrt{1\pm\frac{2}{3}x+x^2}} \\ x &\equiv \frac{B}{B_c}\,, \end{aligned} \tag{4}$$

where B is the magnetic field and B_c is the critical magnetic field for hyperfine decoupling, which is 3.0 kG for $^6\mathrm{Li}^{2+}$. We are not interested in the direction of the electron spin. By assuming the equal probabilities for the initial electron spin states and by taking the sum for the final state, we get

$$\begin{aligned} \begin{pmatrix} P'(|+1>) \\ P'(|\ \ 0>) \\ P'(|-1>) \end{pmatrix} &= \begin{pmatrix} \frac{1}{4}(3+\delta_+^2) & \frac{1}{4}(1-\delta_+^2) & 0 \\ \frac{1}{4}(1-\delta_+^2) & \frac{1}{4}(2+\delta_+^2+\delta_-^2) & \frac{1}{4}(1-\delta_-^2) \\ 0 & \frac{1}{4}(1-\delta_-^2) & \frac{1}{4}(3+\delta_-^2) \end{pmatrix} \begin{pmatrix} P(|+1>) \\ P(|\ \ 0>) \\ P(|-1>) \end{pmatrix} \\ &\equiv D_{1\to 2} \begin{pmatrix} P(|+1>) \\ P(|\ \ 0>) \\ P(|-1>) \end{pmatrix}. \end{aligned} \tag{5}$$

Taking the magnetic field as B=5.0 kG, we obtain the depolarization matrix as

$$D_{1\to 2} = \begin{pmatrix} 0.955 & 0.045 & 0.000 \\ 0.045 & 0.871 & 0.083 \\ 0.000 & 0.083 & 0.917 \end{pmatrix} \equiv D_{\mathrm{dep}}\,. \tag{6}$$

3.2.3 $^6\mathrm{Li}^{2+} \rightarrow {}^6\mathrm{Li}^{3+}$ process

No depolarization takes place.

$$D_{2\to 3} = \mathbf{1}\,. \tag{7}$$

3.3 Depolarization in the charge-exchange (electron capture) process

The lithium ions occasionally capture an electron mainly by the charge-exchange process with the neutral gas in the ECR ionizer. In this process, depolarization which is similar to the one in the ionization process occurs.

3.3.1 $^6\mathrm{Li}^{3+} \rightarrow ^6\mathrm{Li}^{2+}$ process

The spin of the captured electron is randomly oriented. The equation same as Eq. (5) can be applied in this process.

$$D_{3\to 2} = \begin{pmatrix} \frac{1}{4}(3+\delta_+^2) & \frac{1}{4}(1-\delta_+^2) & 0 \\ \frac{1}{4}(1-\delta_+^2) & \frac{1}{4}(2+\delta_+^2+\delta_-^2) & \frac{1}{4}(1-\delta_-^2) \\ 0 & \frac{1}{4}(1-\delta_-^2) & \frac{1}{4}(3+\delta_-^2) \end{pmatrix} = D_{\mathrm{dep}}\,. \tag{8}$$

3.3.2 $^6\mathrm{Li}^{2+} \rightarrow ^6\mathrm{Li}^{1+}$ process

We simply assume that the captured electron quickly de-excites to the $1s$ state and form a spin singlet state with the other electron. In this model, no depolarization of the nucleus occurs.

$$D_{2\to 1} = \mathbf{1}\,. \tag{9}$$

If a meta-stable spin-triplet state is formed, additional depolarization might take place. This effect is not included in the present calculation.

3.3.3 $^6\mathrm{Li}^{1+} \rightarrow ^6\mathrm{Li}^{0+}$ process

The depolarization in this process is negligible since the hyperfine coupling between the captured electron and the nucleus is small.

$$D_{1\to 0} = \mathbf{1}\,. \tag{10}$$

3.4 Depolarization in the atomic excitation and de-excitation process

Lithium atoms and ions are excited by electron impact and spontaneously de-excited to the ground state. The process is considered to proceed quickly comparing with the mixing time among the $|JI>$ states. Hence the nuclear polarization is affected by this atomic excitation and de-excitation process only when the spin orientation of the de-excited electron is opposite in respect to its orientation before the excitation, *i.e.* the electron spin is flipped. Note that atomic meta-stable states are ignored in this model. They might cause additional depolarization effects.

3.4.1 Excitation of $^6\mathrm{Li}^{0+}$

The depolarization in this process is negligible since the hyperfine coupling between the excited electron and the nucleus is small.

$$D_{0\to 0^*} = D_{0^*\to 0} = \mathbf{1}\,. \tag{11}$$

3.4.2 Excitation of $^6Li^{1+}$

In our model, the excited electron of $^6Li^{1+}$ quickly de-excites and forms a singlet state with the other electron. In this case no depolarization takes place.

$$D_{1\to 1^*} = D_{1^*\to 1} = \mathbf{1}\,. \tag{12}$$

3.4.3 Excitation of of $^6Li^{2+}$

The orientation of the spin of the excited electron in $^6Li^{2+}$ may flip during the de-excitation process by the LS coupling between the electron orbital angular momentum and the electron spin.

In a conservative scenario, the spin of the de-excited electron is randomly oriented and the polarization of the nucleus decreases similarly to the ionization process (see Eq. (5)).

$$D_{2\to 2^*} = \mathbf{1}\,, \tag{13}$$

$$D_{2^*\to 2} = \begin{pmatrix} \frac{1}{4}(3+\delta_+^2) & \frac{1}{4}(1-\delta_+^2) & 0 \\ \frac{1}{4}(1-\delta_+^2) & \frac{1}{4}(2+\delta_+^2+\delta_-^2) & \frac{1}{4}(1-\delta_-^2) \\ 0 & \frac{1}{4}(1-\delta_-^2) & \frac{1}{4}(3+\delta_-^2) \end{pmatrix} = D_{\rm dep}\,. \tag{14}$$

It should be noted that about 80% of the initially excited states are the n=2 states ($2s$ or $2p$) [20] (see. Sec. 3.7-(3))) and the probability of the spin-flip of the excited electron during the de-excitation process might be considerably small.

3.5 Depolarization due to the electron spin resonance effect

Free electrons in the ECR ionizer are accelerated by Electron Cyclotron Resonance (ECR) induced by the irradiated microwave. In this ECR region, where the cyclotron frequency and the microwave frequency matches, the electron of $^6Li^{2+}$ ions causes electron spin resonance (ESR) and the orientation of the electron spin is rotated.

In this section, we estimate the rotation angle of the electron spin by the ESR effect in classical formulation.

The ECR ionizer SHIVA is used as a model case. A microwave with a power of 250 W is applied in the ECR chamber which has a cylindrical shape with a diameter of 72 mm. The magnetic field created by the microwave is B_1=0.16 Gauss in the case that the microwave uniformly transmits in the chamber without resonance condition (*i.e.* the chamber does not form a cavity).

In a usual ECR ionizer, the ECR region is located at the surface of an ellipsoid. According to the magnetic field of the SHIVA, the thickness of the ECR region is calculated to be ΔR=4.0 (0.9) μm in the axial (radial) direction at R=5.0 (1.9) cm from the origin. Assuming isotropic distribution of the ion momentum direction, the effective thickness of the ECR region is larger the above thickness by a factor of $\frac{1}{2}(1+\ln\frac{2R}{\Delta R})$. The factor is typically in the region of 5–6. Geometrical average of the effective thickness is about $L \simeq \frac{4.0+0.9\times 2}{3}\times 6$=12 μm.

The rotation angle ($\Delta\omega$) of the electron spin of a $^6Li^{2+}$ ion at T_i=5 eV (v_i=1.3$\times 10^6$ cm/s) during the passage of the 12 μm thick ECR region is

$$\Delta\omega = \gamma_e B_1 \frac{L}{v_i} = 2.8 \times 10^6 \text{ rad}/s \times 9.2 \times 10^{-10} \text{ sec} = 2.6 \times 10^{-3} \text{ rad}\,, \qquad (15)$$

where γ_e=1.76$\times 10^{11}$ rad/sT is the gyromagnetic ratio of the electron. If the ions are confined just in the ECR ellipsoid (this is the worst case) during the confinement time (τ_2=0.66 msec), the number (N) of passages of the ion in the ECR region is

$$N = \frac{v_i \tau_2}{\bar{R}} = \frac{0.66 \times 10^{-3} \text{ sec}}{1.15 \times 10^{-6} \text{ sec}} = 570 \qquad (16)$$

where $\bar{R} \simeq \frac{1}{2}\frac{5.0+1.9\times 2}{3}$ =1.5 cm is the geometrically averaged half-length between the passing points of the ECR region.

The direction of the spin rotation axis in each ESR process randomly changes. The integrated spin rotation angle (ω) is calculated with the random-walk approximation as

$$\omega = \Delta\omega\sqrt{N} = 6.2 \times 10^{-2} \text{ rad} = 3.6^\circ\,. \qquad (17)$$

The result shows that the spin rotation angle of the electron by the ESR effect is negligible. Actually the ions do cyclotron rotations in the magnetic field with a radius of the order of mm. By taking account of this effect, the calculated spin-rotation angle becomes a little bit larger (roughly by a factor of 1.3).

The depolarization of the nuclei is, further, caused by the hyperfine interaction between the electron spin and the nuclear spin. The amount of the depolarization is characterized by $D_{\rm dep}$ even when the spin rotation angle of the electrons is as much as $\omega \sim 2\pi$. Hence we conclude that depolarization of nuclei due to the ESR effect is negligible.

3.6 Depolarization due to the inhomogeneity of the magnetic field

The lithium atoms and ions in the ECR chamber move in an inhomogeneous magnetic field. When the atoms change direction at the wall the rotation of the magnetic field felt by the atoms randomly changes, which cause spin-lattice relaxation of the polarization of the nuclei. Similar effect occurs when ions change their direction at the edge of the plasma region.

This $T1$ relaxation time is discussed by Schearer *et al.* [16], and Cates *et al.* [17]. We should be careful when using the equations in the paper of Cates *et al.* since in some of the equations the factor $(1 + \Omega_0^2\tau_c^2)^{-1}$ is omitted which is important in our case. According to Schearer *et al.*, the $T1$ relaxation time is written as

$$\frac{1}{T1} = \frac{2}{3}\frac{< v^2 >}{\gamma_I^2 \tau_c H_0^4}\left(\frac{\partial H_y}{\partial y}\right)^2\,, \qquad (18)$$

where $< v^2 >$ is the averaged squared velocity of the atoms/ions, γ_I is the gyromagnetic ratio of the ^{6}Li nucleus (by rad/s/T), τ_c is the mean free path, H_0 is the averaged magnetic field, and $\frac{\partial H_y}{\partial y}$ is the averaged magnetic field gradient parallel to the motion.

In the case of lithium ions, by putting the values γ_I=3.94 $\times$ 10^7 rad/s/T, τ_c=1.2 $\times$ 10^{-6} sec, $< v^2 >$=(1.3 $\times$ 10^6 cm/s)^2, H_0=0.5T, $\frac{\partial H_y}{\partial y}$=0.15$T$/cm, we obtain

$$T1 = 4.6 \text{ msec (for ions)} \tag{19}$$

We took the worst case (when the ion moves from the origin in the direction transverse to the symmetry axis and parallel to the sextupole magnetic field) for the field gradient. The relaxation time is comparable with the assumed confinement time of the lithium ions (1 msec for $^6Li^{3+}$). Thus the depolarization of the nuclei in the ions due to the inhomogeneous magnetic field is not negligible. Taking account of the effect that the ions do cyclotron rotation in the magnetic field, the relaxation time is considered to become larger. More realistic calculation is required.

In the case of lithium atoms at the normal temperature, by putting the values γ_I=3.94 $\times$ 10^7 rad/s/T, $< v^2 >$=(9.7 $\times$ 10^4 cm/s)^2, τ_c=3.6 cm/v= 3.7 $\times$ 10^{-5} sec, H_0=0.5T, $\frac{\partial H_y}{\partial y}$=0.3$T$/cm, we obtain

$$T1 = 6.3 \text{ sec (for atoms)} \tag{20}$$

Again we took the worst case for the field gradient. The relaxation time is considered to be much larger than the residence time of the atoms in the plasma chamber, which is estimated as $\ll$ 1 sec. Thus the depolarization of the nuclei in the atoms due to the inhomogeneous magnetic field is negligible.

3.7 Reaction rate of each process

Reaction rate of each process is calculated based on empirical data and fits. Here we list up the numbers and the references.

1. Ionization rates of lithium atoms and ions by electron impact.
   They are calculated by Voronov's empirical fit [18]. Boltzmann distribution of the electron velocity is assumed (T_e=582 eV).

$$\begin{aligned}
\lambda_{0\to1} &= < \sigma_{0\to1} v_e > n_e = 4.52 \times 10^{-8} \mathrm{cm}^3/s \times n_e = 1.01 \times 10^4/s \\
\lambda_{1\to2} &= < \sigma_{1\to2} v_e > n_e = 3.26 \times 10^{-9} \mathrm{cm}^3/s \times n_e = 7.26 \times 10^2/s \\
\lambda_{2\to3} &= < \sigma_{2\to3} v_e > n_e = 7.53 \times 10^{-10} \mathrm{cm}^3/s \times n_e = 1.68 \times 10^2/s
\end{aligned} \tag{21}$$

2. Charge exchange (electron capture) rates of lithium ions with neutral oxygen gas.
   They are calculated by Müller and Saltzborn empirical fit [19]. Boltzmann distribution of the ion velocity is assumed (T_i=5 eV).

$$\begin{aligned}
\lambda_{1\to0} &= < \sigma_{1\to0} v_i > n_{\mathrm{gas}} = 2.14 \times 10^{-9} \mathrm{cm}^3/s \times n_{\mathrm{gas}} = 3.08 \times 10^1/s \\
\lambda_{2\to1} &= < \sigma_{2\to1} v_i > n_{\mathrm{gas}} = 4.81 \times 10^{-9} \mathrm{cm}^3/s \times n_{\mathrm{gas}} = 6.92 \times 10^1/s \\
\lambda_{3\to2} &= < \sigma_{3\to2} v_i > n_{\mathrm{gas}} = 7.72 \times 10^{-9} \mathrm{cm}^3/s \times n_{\mathrm{gas}} = 1.11 \times 10^2/s
\end{aligned} \tag{22}$$

3. Excitation rates of lithium ions by electron impact.
   For $^6Li^{2+}$ they are calculated by Fisher's empirical fit [20]. Boltzmann distribution of the electron velocity is assumed (T_e=582 eV). The excitation rate is larger than the ionization rate by a factor of 2.

$$\lambda_{2\to 2^*} = < \sigma_{2\to 2^*}(n=1\to 2,...,6)v_e > n_e = 1.82\times 10^{-9}\mathrm{cm}^3/s \times n_e = 4.05\times 10^2/s \tag{23}$$

$$\begin{aligned} < \sigma_{2\to 2^*}(n=1\to 2)v_e > &= 1.41\times 10^{-9}\mathrm{cm}^3/s \\ < \sigma_{2\to 2^*}(n=1\to 3)v_e > &= 2.52\times 10^{-9}\mathrm{cm}^3/s \\ < \sigma_{2\to 2^*}(n=1\to 4)v_e > &= 9.32\times 10^{-9}\mathrm{cm}^3/s \\ < \sigma_{2\to 2^*}(n=1\to 5)v_e > &= 4.45\times 10^{-9}\mathrm{cm}^3/s \\ < \sigma_{2\to 2^*}(n=1\to 6)v_e > &= 2.48\times 10^{-9}\mathrm{cm}^3/s \end{aligned} \tag{24}$$

   For $^6Li^{0+}$, the excitation rates are taken from the data of Leep and Gallagher [21]. The excitation rate is larger than the ionization rate by a factor of 10.

$$\lambda_{0\to 0^*} = \sigma_{0\to 0^*}(n=1\to \mathrm{all})v_e n_e = 1.3\times 10^{-8}\mathrm{cm}^3/s \times n_e = 1.0\times 10^5/s \tag{25}$$

   For $^6Li^{1+}$, no data is available. We assumed that the excitation rate is larger than the ionization rate by a factor of 5 taking average of the factors of $^6Li^{0+}$ and $^6Li^{2+}$. This rate is not important for the final result.

$$\lambda_{1\to 1^*} = 5\lambda_{1\to 2} = 3.63\times 10^3/s \tag{26}$$

4. Escape rates.
   Escape rates of ions are simply the inverse of the confinement time.

$$\lambda_{i\to \mathrm{escape}} = \tau_i^{-1} \text{ for } i = 1,2,3 \tag{27}$$

   Since the neutral lithium atom is easily ionized, we used an escape rate of 0 for the neutral ions.

$$\lambda_{0\to \mathrm{escape}} = 0. \tag{28}$$

   The number, $\lambda_{0\to \mathrm{escape}}$, is not important for the final result.

3.8 Simulation and results of the depolarization

The obtained depolarization matrices and reaction rates are summarized in a diagram in Fig. 5. It should be noted that **the depolarization effect due to the inhomogeneity is not included in the present calculation and should be separately considered**.

The diagram is converted to rate equations. The equations are expressed in a form of infinite series of matrices and are analytically solved.

For example, when we feed $^6Li^{1+}$ ions in the plasma chamber with the initial population of the magnetic substates $P_{1+,\mathrm{in}}$, the population of the escaped $^6Li^{3+}$ ions $P_{1+,\mathrm{escape}}$ is calculated as

$$P_{3+,\mathrm{escape}} = \begin{pmatrix} 0.0165 & 0.0010 & 0.0000 \\ 0.0010 & 0.0148 & 0.0017 \\ 0.0000 & 0.0017 & 0.0157 \end{pmatrix} P_{1+,\mathrm{in}} \tag{29}$$

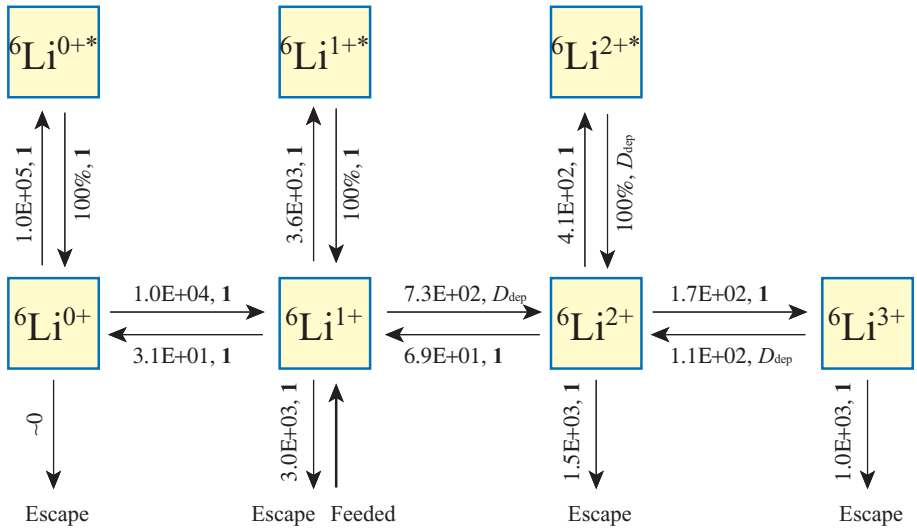

Figure 5: Summary of the reaction rates and depolarization matrices.

From the result, only 1.7% of the fed $^6Li^{1+}$ escape from the plasma region with the charge state of 3+. The polarization of the escaped $^6Li^{3+}$ ions, in the case that the fed $^6Li^{1+}$ ions are in a pure magnetic substate, is summarized in Tab. 2. We see that the depolarization is not very large within the framework of this model while the ionization efficiency is very small.

Table 3 and 4 show the result of the calculation when we assume ten times larger confinement times and ten times larger neutral gas density, respectively. Those two parameters are the ones which are difficult to estimate or measure accurately. In the case that the confinement times are larger by a factor of ten, ionization efficiency increases to 23%, however the reduction of the polarization becomes larger by a factor of two. If the neutral gas density is larger by a factor of ten, the increase of the depolarization is small, but the ionization efficiency becomes smaller by a factor of 1.5.

Again note that the depolarization effect due to the inhomogeneity is not included in the present calculation. The effect is possibly very large if the confinement time is larger by a factor of 10.

From the calculations we conclude that the amount of the depolarization and the ionization efficiency largely depend on the confinement time of the lithium ions and the neutral gas density. The accuracy of the estimation by this simple model calculation is not at the level of detailed discussions but it should be used only to see qualitative features. Therefore, it is crucial to test and measure the numbers in a realistic condition and to study how we can control and optimize those parameters.

Table 2: Calculated depolarization and efficiency for the $^6Li^{1+} \rightarrow {}^6Li^{3+}$ ionization in the ECR ionizer.

Initial State ($^6Li^{1+}$)			Final Sate ($^6Li^{3+}$)		
state	vector pol.	tensor pol.	vector pol.	tensor pol.	efficiency
pure $\mid +1 >$	1.00	1.00	0.94	0.84	0.017
pure $\mid 0 >$	0.00	-2.00	-0.05	-1.54	0.017
pure $\mid -1 >$	-1.00	1.00	-0.90	0.70	0.017

Table 3: Calculated depolarization and efficiency for the $^6Li^{1+} \rightarrow {}^6Li^{3+}$ ionization in the ECR ionizer when the assumed confinement is increased by a factor of 10 (10 msec for $^6Li^{3+}$).

Initial State ($^6Li^{1+}$)			Final Sate ($^6Li^{3+}$)		
state	vector pol.	tensor pol.	vector pol.	tensor pol.	efficiency
pure $\mid +1 >$	1.00	1.00	0.86	0.68	0.23
pure $\mid 0 >$	0.00	-2.00	-0.07	-1.14	0.23
pure $\mid -1 >$	-1.00	1.00	-0.79	0.46	0.23

Table 4: Calculated depolarization and efficiency for the $^6Li^{1+} \rightarrow {}^6Li^{3+}$ ionization in the ECR ionizer when the assumed neutral gas density increased by a factor of ten (1.44×10^{11} cm^{-3}).

Initial State ($^6Li^{1+}$)			Final Sate ($^6Li^{3+}$)		
state	vector pol.	tensor pol.	vector pol.	tensor pol.	efficiency
pure $\mid +1 >$	1.00	1.00	0.94	0.83	0.007
pure $\mid 0 >$	0.00	-2.00	-0.05	-1.53	0.007
pure $\mid -1 >$	-1.00	1.00	-0.90	0.70	0.007

4 Measurements

In the estimation of the degree of depolarization in an ECR plasma, the confinement time is found to be one of crucial parameters. Confinement times of $^6Li^{q+}$ particles have not well understood yet and are main subjects to be studied in this proposal. Measurements will be performed in three steps.

1. Confinement time measurements by the laser ablation method.
2. Confinement time measurements by injecting energetic ^{6}Li ions into an ECR plasma.
3. Polarization measurements of $^6Li^{3+}$ ions after ionization.

The RIKEN 18 GHz superconducting ECRIS [22] is used for these experiments. The source has auxiliary coils to modify magnetic field profiles by mirror coils. The ion confinement time and ionization efficiency are expected to be sensitive to the mirror ratio of the ECR ion source. By the laser ablation method, we can measure confinement times of ions when ^{6}Li atoms are introduced in the ECR plasma. This situation is different from the proposed source, but is expected to provide the basic information on the ECR plasma as well as a kind of the standard by comparing with previous results on Al [14]. All the required equipments exist and no additional budget is needed.

The second experiment is important to estimate depolarization effects anticipated for the proposed ion source. Ion confinement times and yields are investigated with changing magnetic field profiles, deceleration voltage, vacuum pressures of the plasma region, etc. It is necessary to prepare for a Li oven, a surface ionizer, an acceleratation and focusing electrodes, an insulation of the plasma chamber to change the incident energy of $^6Li^{1+}$ ions into the ECR plasma, see Fig. 4. There are some reports on charge breeders for heavy ions [23, 24, 25], but have been no measurements on ^{6}Li ions.

Polarization of $^6Li^{3+}$ is measured after acceleration by the AVF cyclotron. The tensor analyzing power, A_{yy}, of the ^{2}H(^{6}Li,^{4}He)^{4}He reaction can be known from the data of the inverse kinematic reaction using a tensor polarized deuteron beam. For this experiment, we need optical pumping system including two diode lasers. We prefer a diode laser to a dye laser pumped by an Ar laser. The latter requires annual maintenance of the Ar laser.

Finally, the budget request is summarized below.

Second step	Li oven	2,000,000
	acceleration system	1,000,000
	electro-static lenses, insulations	1,000,000
	Subtotal	4,000,000
Third step	diode lasers ($\times$ 2)	8,000,000
	optical components	2,500,000
	Subtotal	10,500,000
	Total	14,500,000

We would like to begin the first measurement this winter.

References

[1] H. Yukawa, Proc. Phys. Math. Soc. Jpn 17 (1935) 48.
[2] H. Okamura *et al.*, Phys. Rev. C **66** (2002) 054602.
[3] U. Holm *et al.*, Z. Phys. **233** (1970) 415.
[4] E. Steffens *et al.*, Nucl. Instrum. Methods **124** (1975) 601.
[5] E. Steffens *et al.*, Nucl. Instrum. Methods **143** (1977) 409.
[6] G.S. Masson *et al.*, Nucl. Instrum. Methods in Phys. Res. A **242** (1986) 196.
[7] O. Karban *et al.*, Nucl. Instrum. Methods in Phys. Res. A **274** (1989) 4.
[8] H. Reich and H.J. Jänsch, Nucl. Instrum. Methods in Phys. Res. A **288** (1990) 349.
[9] E.G. Myers *et al.*, Nucl. Instrum. Methods in Phys. Res. B **79** (1993) 701.
[10] P.A. Chamouard *et al.*, Colloque de Physique, Colloque C6, supplement au n°22 (1990) C6-565.
[11] T. Kurita *et al.*, Rev. Sci. Instrum. **71** (2000) 909.; M. Imanaka *et al.*, Rev. Sci. Instrum. **73** (2002) 592.;
[12] T. Nakagawa *et al.*, Rev. Sci. Instrum. **73** (2002) 513.
[13] P. Ludwig *et al.*, Rev. Sci. Instrum. **69** (1998) 653.
[14] M. Imanaka, PhD thesis, Universitiy of Tsukuba, unpublished.
[15] Shirkov, CERN/PS 94-13.
[16] L.D. Schearer and G.K. Walters, Phys. Rev. **139** (1965) A1398.
[17] G.D. Cates, *et al.*, Phys. Rev. A **37** (1988) 2877.
[18] G.S. Voronov, Atom. Data. Nucl. Data Tables **65** (1997) 1.
[19] A. Müller and E. Slazborn, Phys. Lett. A **62** (1977)391.
[20] V. Fisher *et al.*, Phys. Rev. A **55** (1997) 329.
[21] D. Leep and A. Gallagher, Phys. Rev. A **10** (1974) 1082.
[22] T. Nakagawa *et al.*, 9th Int. Conf. on Ion Sources, LBNL, Oakland, USA Sept. 2001.
[23] R.C. Pardo *et al.*, Rev. Sci. Instrum. **67** (1996) 1602.
[24] N. Chauvin *et al.*, Nucl. Instrum. Methods in Phys. Res. A **419** (1998) 185.
[25] P. Sortais *et al.*, Nucl. Phys. A **701** (2002) 537c.